Quiescent Crystallization Kinetics and Morphology of Isotactic Polypropylene Resins for Injection Molding. I. Isothermal Crystallization

B. DE CARVALHO, R. E. S. BRETAS

Department of Materials Engineering, UFSCar, 13565-905 São Carlos, SP, Brazil

Received 7 July 1997; accepted 5 October 1997

ABSTRACT: The quiescent isothermal crystallization kinetics of polypropylene was studied as a function of molecular weight (M_w), amount of ethene, and amount of maleic anhydride and acrylic acid grafting. Differential scanning calorimetry and polarized light optical microscopy were used to follow this kinetics. It was observed that the linear growth rate, G, decreased with the increase of M_w, but increased with the amount of ethene. In the grafted polymers, as the amount of grafting increased, G decreased. The fold surface free energy, σ_e, was found to increase with the increase in M_w. The heterophasic and grafted polymers had σ_e values higher than the homopolymers. All samples showed spherulitic morphology, except the acrylic acid-grafted polypropylene that showed axialitic morphology. © 1998 John Wiley & Sons, Inc. J Appl Polym Sci 68: 1159–1176, 1998

Key words: polypropylene; crystallization kinetics; fold surface free energy; heterophasic polypropylene; grafted polypropylene

INTRODUCTION

Isotactic polypropylene (iPP) resins are extensively used in all kind of products, from lawn furniture, bicycle wheels, and latex paints to automotive parts.[1] Usually, these products are made by injection molding, in which high pressures and high shear and elongational rates are applied to force the polymer toward a cavity. The cavity is at a lower temperature (usually below the glass transition temperature, T_g, of the polymer) than the melt. Therefore, crystallization will occur under high pressures, high temperature gradients, and high deformational rates. Because final crystallinities and morphology are the determinant factors that influence mechanical properties of these products, the prediction of both parameters constitutes an advance in the optimization of the injection-molding process.

Isayev and coworkers[2,3] have studied and simulated the crystallization gradients that are found in an injection-molded sample (dumbell-shaped) made of iPP, of average molecular weight equal to 3.51×10^5 g gmol^{-1}. To perform this simulation, they assumed that the highly oriented lamellar morphology near the wall of the mold was the result of shear-induced crystallization, whereas the spherulitic morphology in the center of the mold was due to quiescent crystallization. The shear-induced crystallization was modeled by using the Eder–Janeschitz–Kriegl–Liedauer,[4] whereas the quiescent crystallization was modeled by using a Nakamura-type equation. Their results showed that the rate of shear-induced crystallization was higher than of the quiescent crystallization.

The quiescent crystallization of iPP has been widely studied. Clark and Hoffman[5] observed that, at large undercoolings, the growth rate, G, showed an abrupt upward trend, a departure from the straight-line behavior observed at low under-

Correspondence to: R. E. S. Bretas (bretas@power.ufscar.br).

Journal of Applied Polymer Science, Vol. 68, 1159–1176 (1998)
 CCC 0021-8995/98/071159-18

coolings. They analyzed iPP experimental crystallization data of other authors and showed that these data were consistent with the surging of a transition between regime II and regime III of crystallization that occurred at 137°C. The average fold surface free energy, σ_e, was found to be 65–70 erg cm^{-2}. This transition was also found to be technologically important because products are usually crystallized in regime III; therefore, the morphology formed at this regime as given by the theory of Hoffman and coworkers[6] is expected to be extremely rough due to the intense multiple nucleation that occurs, with a high degree of loops and tie molecules that will influence the toughening properties of the polymer.

Varga[7] also made an excellent review of the supermolecular structure of iPP that is formed after quiescent isothermal and nonisothermal crystallization. He observed that, if the isothermal crystallization temperature, T_c, is varied (or also if the cooling rate α is varied), a wide range of structures is formed, from α-modified at low and high undercoolings to a mixture of α- and β-modified at intermediate undercoolings. The reduction of the crystallization temperature or the increase of the cooling rate decreased the average spherulite size. Above 140°C, the growth rate of the α-modification exceeded that of the β-modification. The α- and β-modifications proceeded in regimes II and III; the transition of regimes II to III of the α-modification occurred at 135°C, whereas that of the β-modification occurred at 133°C. Above 141°C, theoretically, no β-modification structure was formed.

Varga[7] also pointed out that the spherulitic crystallization of block ethylene/propylene copolymers with low ethylene content is different from those of the iPP homopolymers: on the surface of the copolymer spherulites, a fine distribution of droplike inclusions, approximately 1 μm of diameter, was observed. These inclusions were attributed to the phase separation of crystallized chain

Table I PP Resins Used in This Work

	Homopolymer		
Sample	M_w (g gmol^{-1})	MFI (g 10 min^{-1})	
H1	84,000	756.00	
H2	240,000	18.00	
H3	416,000	2.4	
H4	470,000	1.5	
H5	1,400,000	0.03	
	Heterophasic		
	Percent Ethene (in the Synthesis)	MFI (g 10 min^{-1})	Percent Ethene Copolymer–Rubber
C1	6.8	5.7	
C2	10.3	5.7	
C3	13.0	5.4	6.4–38.3
C4	9.0	1.0	
	Grafted		
	Percent (w/w) MA (Final)	Percent (w/w) AA (Final)	MFI (g 10 min^{-1})
PPgAM1	0.18		190.0
PPgAM2	0.54		4.7
PPgAM3	0.18		5.0
PPgAA		6.0	

MFI, melt flow index; MA, maleic anhydride; AA, acrylic acid.

segments of ethylene sequences. In a more recent paper,[8] it was found that the G of iPP decreased with the increase in the addition of an ethylene-α-olefin copolymer fraction with 50.5 mol % of 1-hexene, when both polymers were blended. This effect was attributed to their miscibility.

Lim and coworkers[9] also pointed out that the crystallization of iPP is a nucleation-controlled process in which all nuclei are formed simultaneously. They studied the effect of a nucleating agent on the overall crystallization growth rate and concluded that its addition reduced this rate; the found value of σ_e agreed well with the literature. They also attributed the lower value of σ_e of the nucleated compositions relative to the nonnucleated to the formation of loops and dangling chains ends in the nucleated lamellae.

Hieber[10] also made an extensive review of the methods used on calculating data for the isothermal crystallization of iPP, from 1959 to 1993. He found that the usual experimental methods used for this calculation were dilatometry and differential scanning calorimetry (DSC). The T_cs range was between 62 and 160°C. Also, he found that the values of the Avrami parameter, n, varied from 1.8 to 7.6. He pointed out after analyzing all of these data that the observed large scatter was due to uncertainties or inaccuracies in the experimental measurements. For example, he observed that, in one case, the light depolarizing microscopy technique gave faster kinetics than the DSC. However, in another case, when both techniques were used, the two types of measurements agreed quite well. This observation was already highlighted by Wunderlich,[11] who stated that, without the parallel knowledge of microscopy results, the Avrami plots obtained by DSC data were the only convenient means to represent the empirical data of crystallization.

Regarding the influence of molecular weight, it has been found,[12] as in other polymers,[13] that the G of iPP decreases with the increase in the number average molecular weight (M_n). However, in a more recent and comprehensive study made by Misra and coworkers[14] on this subject, the authors found that increasing the weight average molecular weight (M_w) for a given polydispersity increased the overall crystallization rates. It is worthwhile to point out that Hoffman and Miller,[15] using the reptation concept, predicted that G would be inversely proportional to M_w. One work,[16] however, concluded that there was no dependence of G on M_w. An old study[17] with polysiloxane indicated that, above certain M_w, G was independent of M_w.

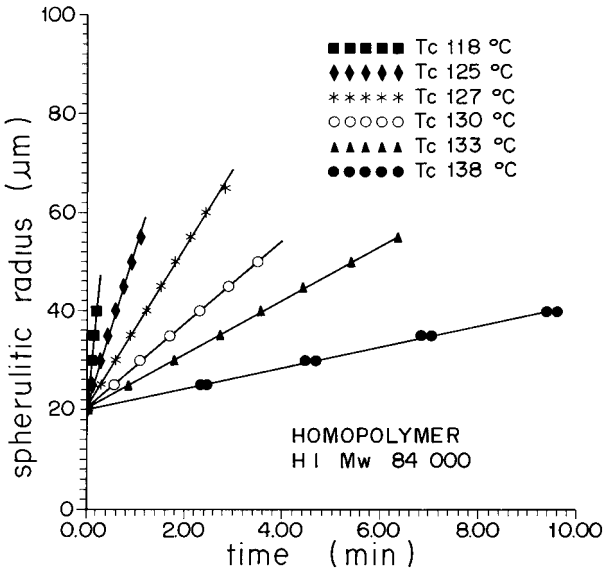

Figure 1 Standard spherulite radius versus time curves for the homopolymers, at different T_cs.

As it can be seen, extensive research has been made on the quiescent crystallization of iPP; however, in injection molding, the crystallization is nonisothermal, and it occurs at extremely high cooling rates. Evidently, the experimental reproduction of these conditions is extremely difficult to achieve.

The main objective of this work is to develop an empirical constitutive equation for the quiescent nonisothermal crystallization of various PP resins that are commonly used in injection molding, as a function of M_w, amount of ethene, and amount of grafting. This equation will be used later for simulation of the postfilling stages of an injection-molding process.

In the first part of this work, we will present data of the quiescent isothermal crystallization and the resulting morphology. In the second part, we will present data on the quiescent nonisothermal crystallization and resulting morphology. Finally, in the third part, we will formulate the constitutive equation for crystallization, and we will use it in the simulation of the postfilling stages of the injection molding of these polymers into a rectangular mold.

EXPERIMENTAL

Materials

The polypropylene (PP) resins were kindly donated by OPP Petroquimica do Brasil. The grades used are listed in Table I.

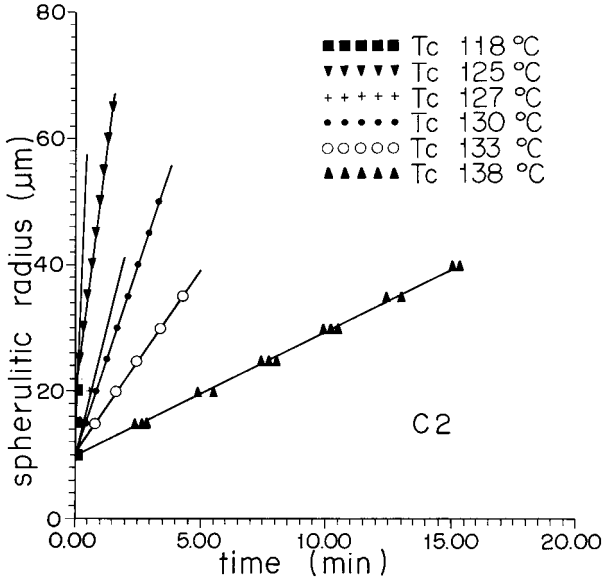

Figure 2 Standard spherulite radius versus time curves for the heterophasic polymers, at different T_cs.

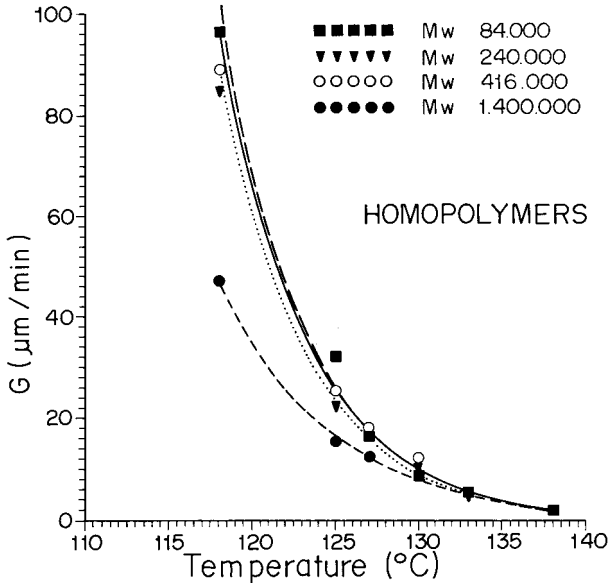

Figure 4 Growth rate, G, of the homopolymers as a function of temperature.

Isothermal Crystallization

The growth rate of crystallization G was measured by using a polarized light optical microscope, PLOM, Leica, model DMRXP and a hot stage, from Linkam, model THMS 600. To this microscope, a video camera Kappa, was attached and the spherulitic growth of the samples recorded by video equipment. Therefore, the spherulite diameters were measured directly from the videotapes. The samples were melted at 200°C, for 5 min (except sample H5, melted at 220°C), and then cooled down, at -100°C min^{-1} to the

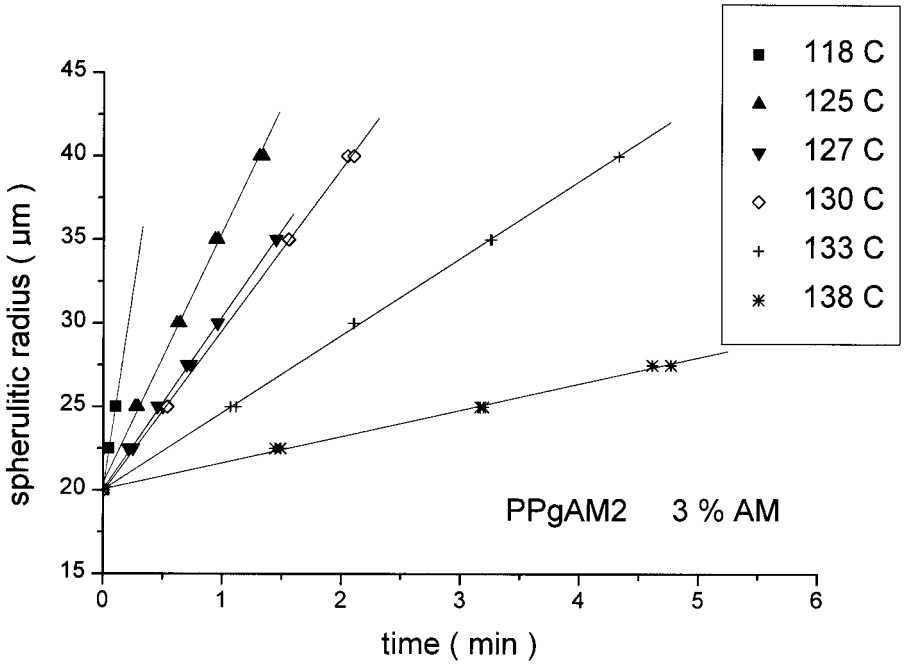

Figure 3 Standard spherulite radius versus time curves for the grafted polymers, at different T_cs. AM, maleic anhydride.

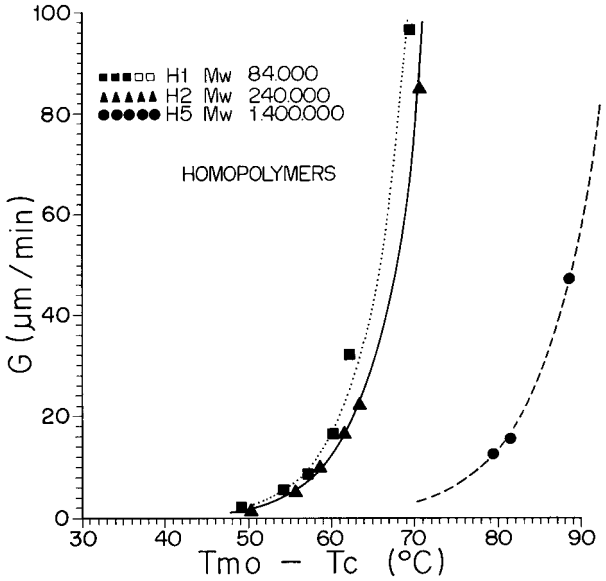

Figure 5 Growth rate, G, of the homopolymers as a function of degree of undercooling.

following crystallization temperatures: 138°, 133°, 130°, 127°, 125°, and 118°C. The growth rate of each sample was calculated by measuring the slopes of the spherulite radius versus time curves.

To complement these optical data, thermal data were also obtained by using a DSC (DSC-7 from Perkin-Elmer, Norwalk, CT) with a nitrogen atmosphere. The samples were heated at 20°C min^{-1} up to 200°C, maintained at this temperature for 5 min, and then cooled down to the abovementioned crystallization temperatures. After each isothermal run was completed, the samples were again heated at 10°C min^{-1} until their melting temperatures, T_m, were observed. These melting temperatures were used to calculate the equilibrium melting temperature, T_m^o, of the polymers, by using the procedure by Hoffman and colleagues.[6]

The glass transition temperature, T_g, was measured by using a dynamic mechanical analyzer (DMTA) from Polymer Labs; on the bending mode, double cantilever, at 1 Hz, and 64 μm of strain. The samples were heated at 4°C min^{-1}. T_g was assumed to be the temperature at which the loss modulus, E'', had a maximum.

Morphology

The final morphology of the PLOM samples was also observed by using a scanning electron microscope from Carl Zeiss, model 940-A, after coating with gold by vacuum metallization. The rubber particles in the heterophasic samples had their average sizes, average areas, and size distribution analyzed by using a MOCHA software, 1.2.10 version, from Jandel Scientific (Corte Madera,

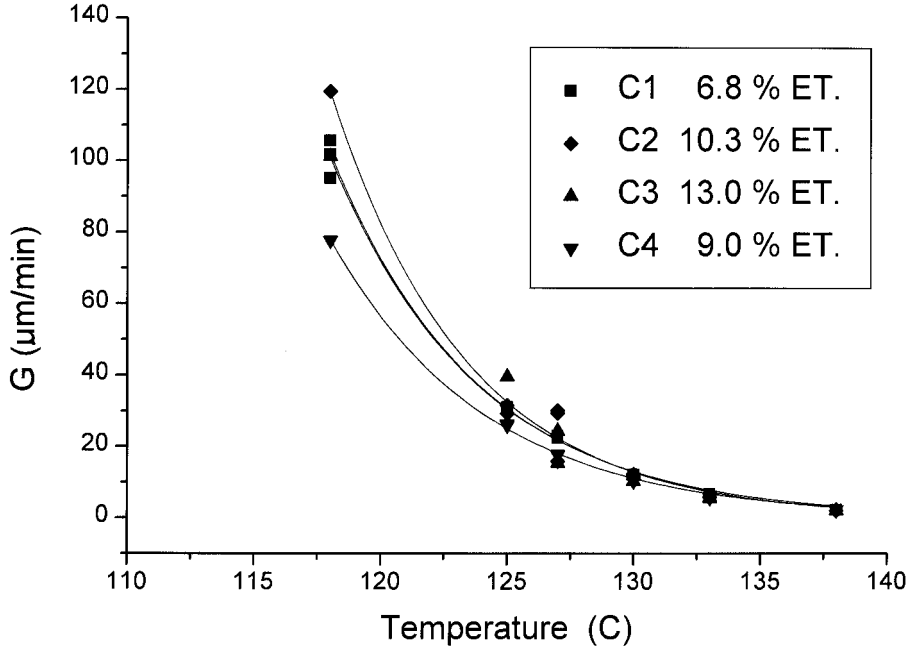

Figure 6 Growth rate, G, of the heterophasic polymers as a function of temperature. ET, ethene.

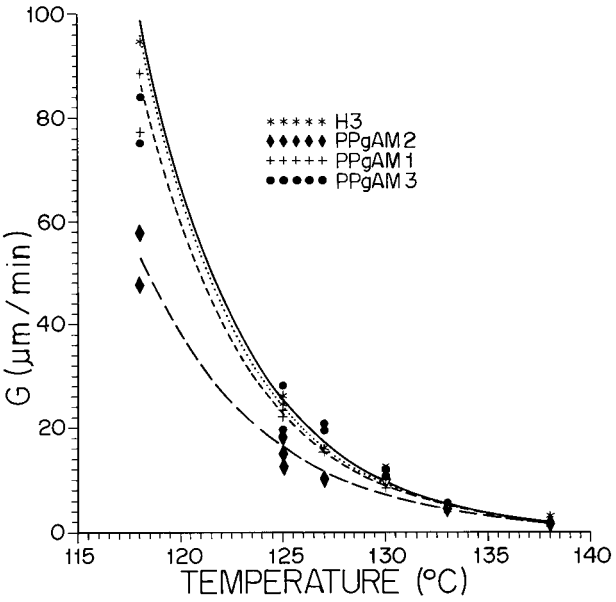

Figure 7 Growth rate, G, of the grafted polymers as a function of temperature.

CA), after removing the elastomeric phase with a chromic acid solution (H_2SO_4, H_3PO_4, H_2O, and CrO_3), at 60°C for 5 min.

RESULTS AND DISCUSSION

Isothermal Crystallization

Figures 1–3 show standard curves of the spherulite radius, r_e, versus time of the homophasic, heterophasic, and grafted polymers, at different T_cs. It can be observed that the radius has a linear dependence with time at all T_cs, showing that the spherulite growth was not controlled by diffusion, even at the final crystallization stages. A nonlinear growth rate could be expected to be observed in the heterophasic polymers, if the rubber phase, mainly ethylene–propylene rubber (EPR) would diffuse away radially more rapidly than the PP spherulite growth, therefore changing the composition of the growth front[18]; however, because a constant radial growth was observed, we concluded that this rejection did not occur. We would also expect that the EPR particles will be trapped within the PP spherulites.

The linear growth rate $G = dr_e/dt$; these values are shown as a function of temperature in Figures 4–7. Figure 4 shows G for the homopolymers; as

Table II Values of T_m^o and T_g of the Samples Used in This Work

Samples	T_m^o (°C)	T_g (°C)
H1	187.2	—
H2	188.4	2.16 (0.47)
H5	206.3	—
C1	200.3	6.31 (0.46)
C2	196.9	4.86 (1.79)
C3	205.4	6.45 (0.40)
C4	201.3	6.05 (0.38)
PPgAM2	209.2	3.34 (0.02)
PPgAM3	—	7.50 (1.04)

Numbers in parentheses represent standard deviations.

expected, G decreases with the increase in M_w. These data are also plotted as a function of the degree of undercooling, $\Delta T = T_m^o - T_c$, for samples H1, H2, and H5, and are shown in Figure 5. As expected, as the degree of undercooling increases, G also increases. Table II shows the values of T_m^o, calculated by DSC and the Tg's calculated by DMTA. The relationship between T_m and T_m^o is given by Hoffman and coworkers,[6] or

$$T_m = T_m^o(1 - 2\sigma_e/l\Delta H_m) \quad (1)$$

where l is thickness of the lamella and ΔH_m is heat of fusion per unit volume of crystal.

A plot of T_m versus $1/l$ is linear and has an intercept of T_m^o, where $1/l \to 0$. However, if we consider that the crystals formed at T_c thicken with time by some factor β, then eq. (1) can be expressed as

$$T_m = T_m^o(1 - 1/\beta) + T_c/\beta \quad (2)$$

and T_m^o can be determined from a plot of T_m versus T_c where T_m^o is the intercept of the extrapolated T_m values and a line defined by $T_m = T_c$.

We can also relate T_m^o with the amount of comonomer and molecular weight, by an expression given by Sperling[19]:

$$(1/T_m) - (1/T_m^o) = (R/\Delta H_m)X_b = (R/\Delta H_m)(2M_o/M_n) \quad (3)$$

where X_b is the mole fraction of the noncrystalliz-

Figure 8 Hoffman and Lauritzen plots from eq. (5) for the polymers: (a) homopolymer H2; (b) homopolymer H5; (c) PPgAM2; (d) heterophasic C2; and (e) heterophasic C3.

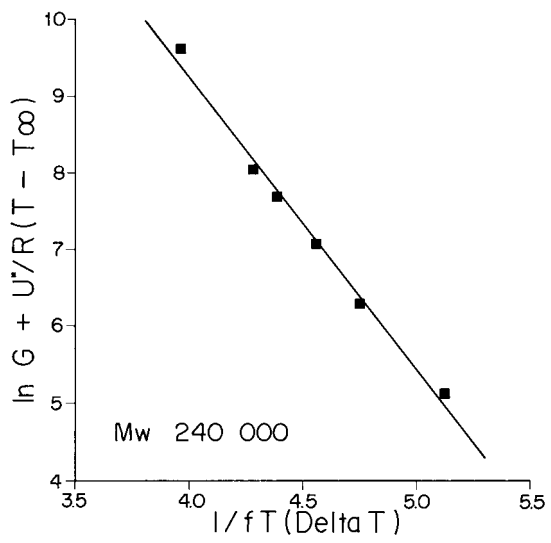
ln G + U*/R(T − T∞)
Mw 240 000
1/fT(DeltaT)

(a)

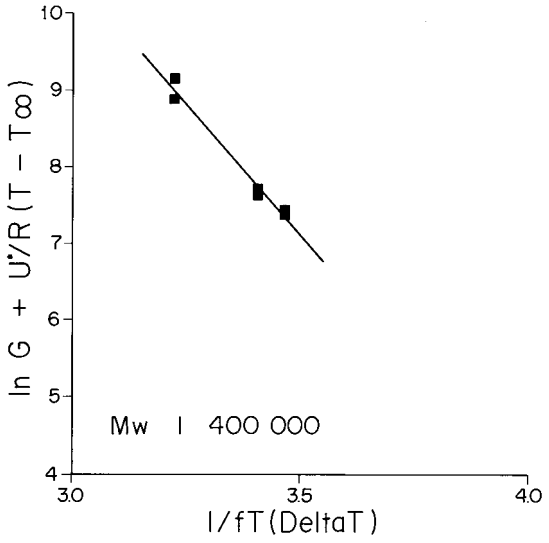
ln G + U*/R(T − T∞)
Mw 1 400 000
1/fT(DeltaT)

(b)

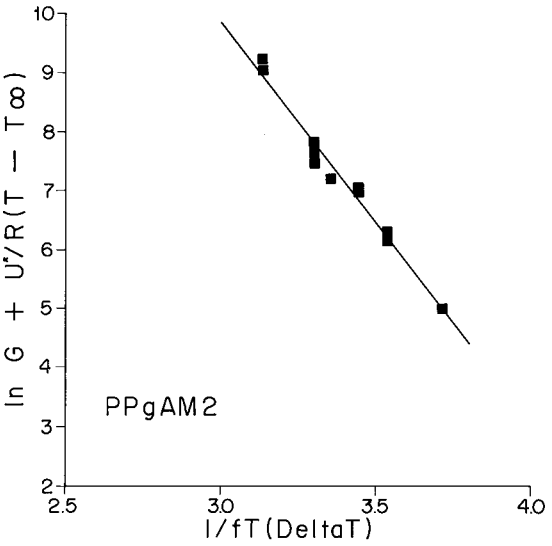
ln G + U*/R(T − T∞)
PPgAM2
1/fT(DeltaT)

(c)

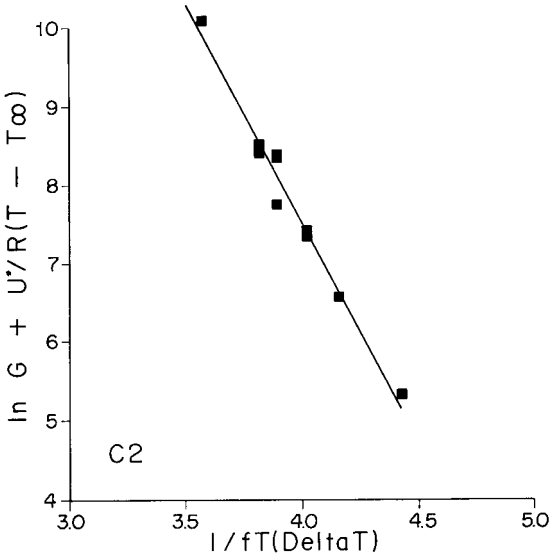
ln G + U*/R(T − T∞)
C2
1/fT(DeltaT)

(d)

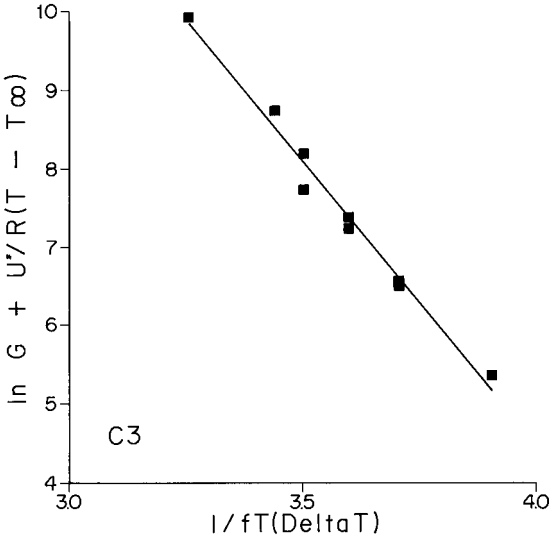
ln G + U*/R(T − T∞)
C3
1/fT(DeltaT)

(e)

Table III Calculated Values of the Fold Surface Free Energy, σ_e

Sample	$\sigma\sigma_e$ (erg cm^{-2})	σ_e (erg cm^{-2})	q (kcal mol^{-1} of folds)	G_o (μm min^{-1})
H1	862	75	7.742	3.505×10^{10}
H2	893	78	7.712	4.257×10^{10}
H5	1537	134	13.250	2.788×10^{13}
C1	1371	119	11.767	1.695×10^{13}
C2	1274	111	10.976	7.508×10^{12}
C3	1622	141	13.942	2.688×10^{14}
C4	1302	113	11.173	3.720×10^{12}
PPgAM2	1536	134	13.250	1.700×10^{13}

able comonomer, M_o is the molecular weight of an end mer, and R is the gas constant.

It can be observed that, as expected, T_m^o increases with the increase in molecular weight. The behavior of the heterophasic polymers is more difficult to explain. Usually, the amount of ethene in the copolymer matrix is small; for example, in sample C3, 6.4% of the total amount of ethene is known to be incorporated randomly in the copolymer chain backbone. Therefore, because they all are synthesized in the same way, we can assume that samples C1 and C2 have, respectively, approximately 3 and 5% of the total amount of ethene in the copolymer chain backbone. In this way, we can compare samples C1 and C2 (same molecular weight): the increase in the amount of ethene decreased T_m^o as expected by eq. (3). Comparing samples C2 and C3, we can observe that sample C3 has a higher molecular weight than C2; therefore T_m^o will increase.

In the case of the grafted polymer, the high value of T_m^o can be credited, in part, to its high molecular weight.

Figure 6 shows G as a function of temperature for the heterophasic resins. If we analyze two samples with the same melt flow index (C1 and C2), for example, we can observe that the sample with the highest amount of ethene, C2, presents a higher G. Because both samples presented a linear spherulitic growth, we can assume that, as described previously, the composition of the crystallization front was constant, because the crys-

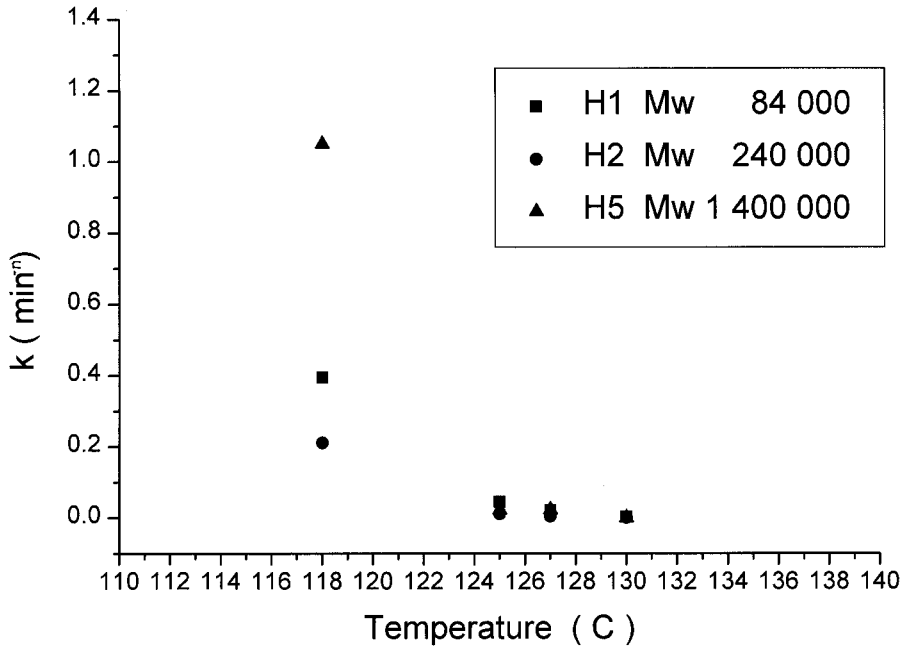

Figure 9 Avrami parameter k of the homopolymers as a function of temperature.

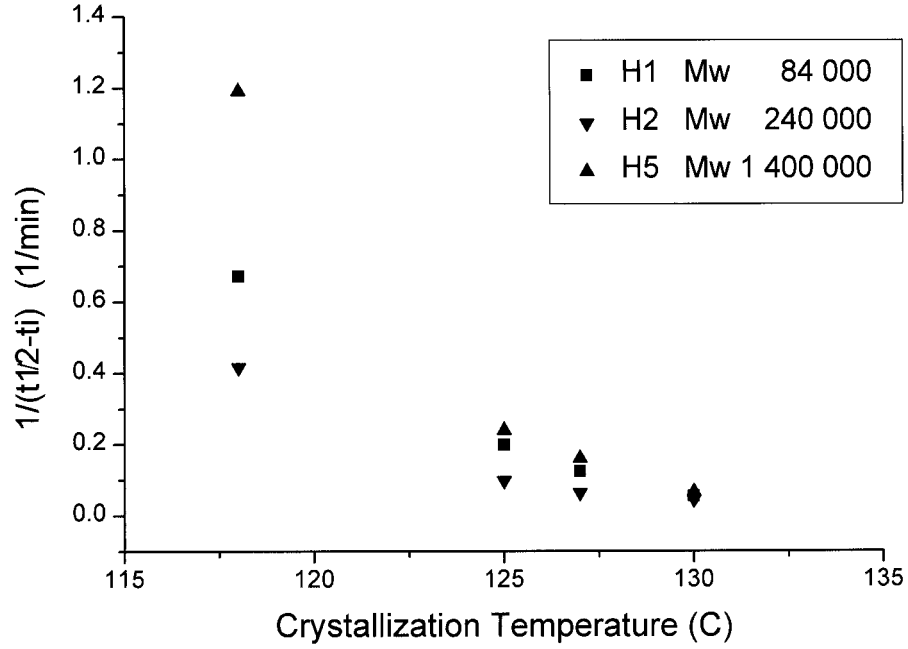

Figure 10 $1/(t_{1/2} - t_i)$ of the homopolymers as a function of temperature.

tallization rate of the PP outstripped the rate at which the EPR particles diffused away. However, in the case of sample C2, because it has a higher amount of ethene (and probably a higher amount of EPR and a higher amount of ethene in the copolymer matrix), probably the EPR particles acted as nucleation agents or then the ethene portion of the copolymer chain helped to flexibilize the whole chain, making easier the diffusion from the melt to the substrate. In any case, the overall crystallization rate would be accelerated. Regarding samples C3 and C4, both have higher M_w than

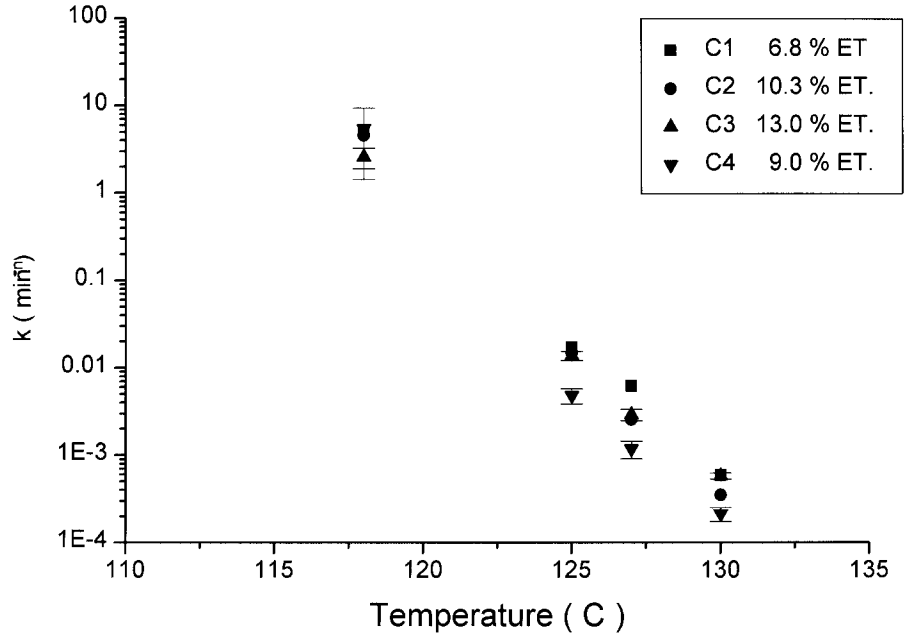

Figure 11 Avrami parameter k of the heterophasic polymers as a function of temperature. ET, ethene.

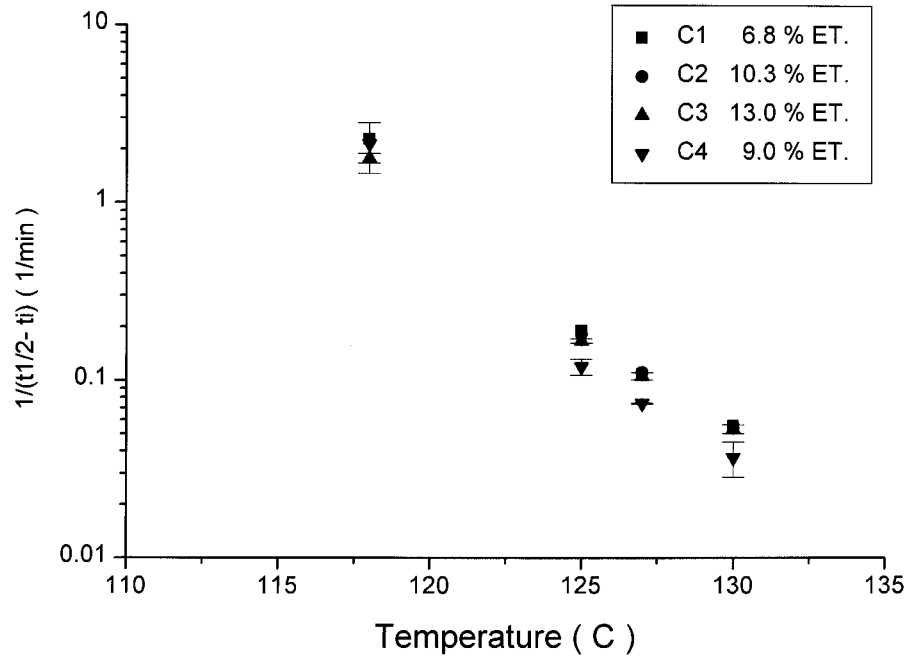

Figure 12 $1/(t_{1/2} - t_i)$ of the heterophasic polymers as a function of temperature. ET, ethene.

samples C1 and C2; therefore, their growth rates decreased because their M_w increased, as observed in Figure 4. In this case, the influence of the M_w on G outstripped the influence of the amount of ethene (or EPR).

Figure 7 shows G as a function of temperature for the grafted polymers. The virgin polymer was resin H3; it can be seen that, as the percent of grafting increases, G decreases. Sample PPgAM2, that had the highest M_w, also had the lowest G

Table IV Avrami Parameter *n* of the Samples

Sample	T_c (°C)	n	Sample	T_c (°C)	n
H1	118	1.50 (0.10)	H2	118	1.44 (0.07)
	125	1.69 (0.03)		125	1.77 (0.31)
	127	1.67 (0.06)		127	1.3 (0.1)
	130	2.0		130	2.0
H5	118	2.13 (0.02)	C1	118	2.4
	125	2.4		125	2.2
	127	2.45		127	2.13
	130	2.68		130	2.45
C2	11	2.34	C3	118	2.3 (0.12)
	125	2.28		125	2.17 (0.16)
	127	2.55		127	2.46 (0.01)
	130	2.61		130	2.42 (0.01)
C4	118	2.45 (0.08)	PPgAM	125	1.76
	125	2.37 (0.04)		127	1.94
	127	2.46 (0.10)		130	2.00
	130	2.46 (0.11)		133	1.87
PPgAA	130	1.95			
	133	2.24			
	138	2.28			
	142	2.31			

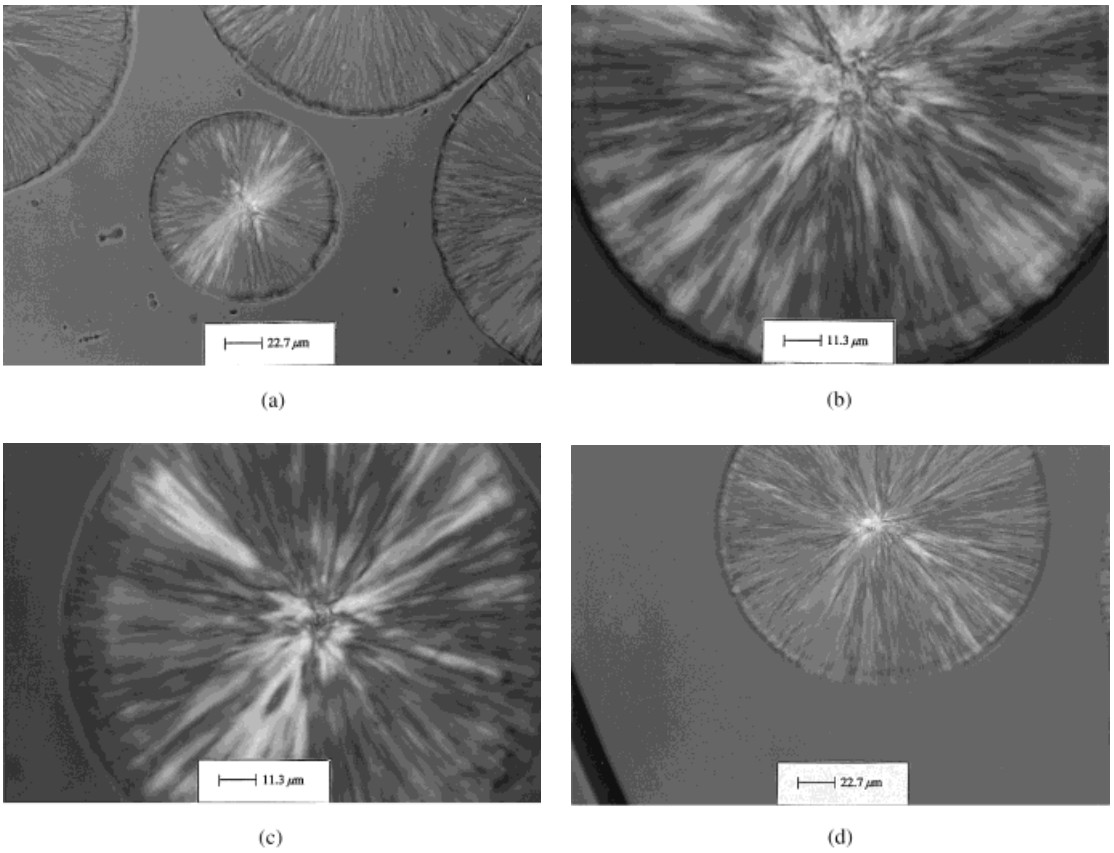

Figure 13 PLOM of some of the homopolymers after isothermal crystallization at different T_cs: (a) sample H1, T_c = 130°C, ×200; (b) sample H2, T_c = 135°C, ×400; (c) sample H4, T_c = 138°C, ×400; (d) sample H5, T_c = 125°C, ×200.

value. It seems that the percent of grafting has more influence on G than the M_w, because the difference in M_w between samples PPgAM2 and PPgAM3 is small; however, their G values are very different. The percent of grafting of the PPgAM2 is almost $2\frac{1}{2}$ times the percent of grafting of PPgAM3. It is important to point out that the amount of MA that it is grafted is also very small (0.1 and 0.54% w/w); however it seems to affect G extensively. Depending on the process conditions (temperature, amount of peroxide, extrusion velocity, etc.), the peroxide can also break the PP chain, therefore increasing its molecular weight distribution; also, a high amount of residual maleic anhydride can remain in the melt. These two factors can explain the high value of melt flow index of sample PPgAM1 after the reactive extrusion.

Data on the PPgAA were not collected because this polymer showed an extremely high nucleation rate. Also, there was no formation of spherulite morphology; instead, a needlelike structure was observed.

The value of G was also calculated by using the traditional equation by Hoffman and coworkers[6]:

$$G = G_o \exp[-U^*/R(T_c - T_\infty)] \exp[-K_g/T_c(\Delta T)f] \quad (4)$$

where G_o is preexponential factor (independent of temperature), U^* is activation energy for reptation in the melt = 1500 cal mol^{-1}, T_∞ is theoretical temperature at which reptation ceases $= T_g - 30K$, K_g is nucleation constant, ΔT is degree of undercooling, and f is $2T_c/T_m^o + T_c$.

This equation can also be written as

$$\ln G = \ln G_o - U^*/R(T_c - T_\infty) - K_g/T_c(\Delta T)f \quad (5)$$

Therefore, if we plot $[\ln G + U^*/R(T_c - T_\infty)]$ as

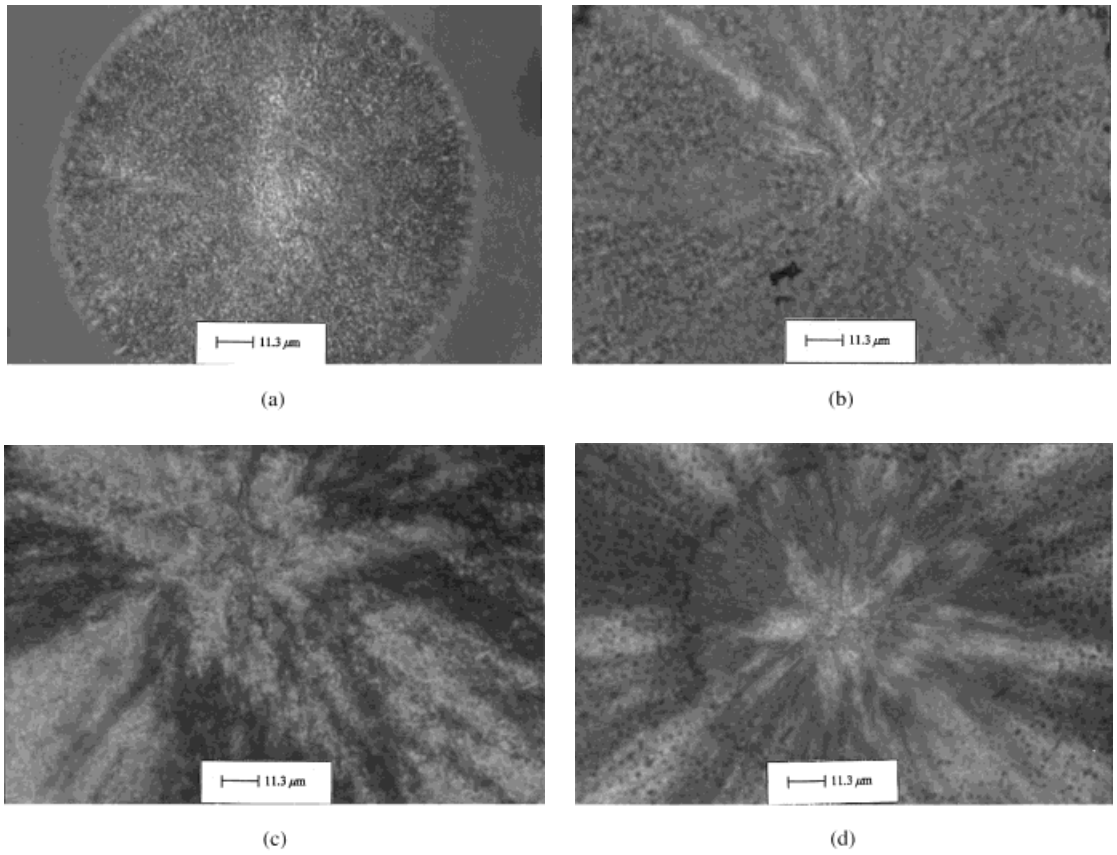

Figure 14 PLOM of some of the heterophasic polymers, after isothermal crystallization, at different T_cs: (a) sample C1, T_c = 130°C, ×400; (b) sample C2, T_c = 125°C, ×400; (c) sample C3, T_c = 127°C, ×400; (d) sample C4, T_c = 138°C, ×400.

a function of $1/T_c(\Delta T)f$, and a straight line is obtained, this result will indicate that eq. (5) can describe with some precision the experimental G as a function of temperature. These plots are shown in Figure 8 for some of the polymers. It can also be observed that all of the experimental data can be adjusted by straight lines; therefore, the Hoffman and Lauritzen equation can describe with precision this crystallization kinetics.

No transition between regimes II and III was observed, as pointed out by Clark and Hoffman,[5] probably because our maximum T_c was 138°C, very close to the transition temperature observed by these authors.

From the slopes of these lines, we can calculate K_g and consequently σ_e, the fold interfacial free energy, if σ, the lateral surface interfacial free energy is known, because

$$K_g = rb\sigma\sigma_e T_m^o / \Delta H_m^o k \qquad (6)$$

where r is the parameter characteristic of the growth regime (its value will be 4 if the regimes are I or III and 2 if the regime is II), b is the thickness of the surface nucleus, ΔH_m^o is the equilibrium heat of fusion, and k is the Boltzmann constant.

The main contribution to σ_e is the necessary work to fold the polymeric chain or work of folding, q, given by

$$q = 2\sigma_e ab \qquad (7)$$

where a is the width of the molecular chain.

The following values[5] were used for the calculation: b is 6.26×10^{-8} cm, a is 5.49×10^{-8} cm (110 growth plane), ΔH_m^o is 1.96×10^9 erg cm^{-3}, σ is 11.49 erg cm^{-2}, and r is 4 (regime III).

Table III presents these results. It can be observed that samples H1 and H2 have similar σ_e; however, sample H5 has a higher σ_e. H5 also has the highest M_w of all the polymers used in this study. Clark and Hoffman[5] estimated, from data

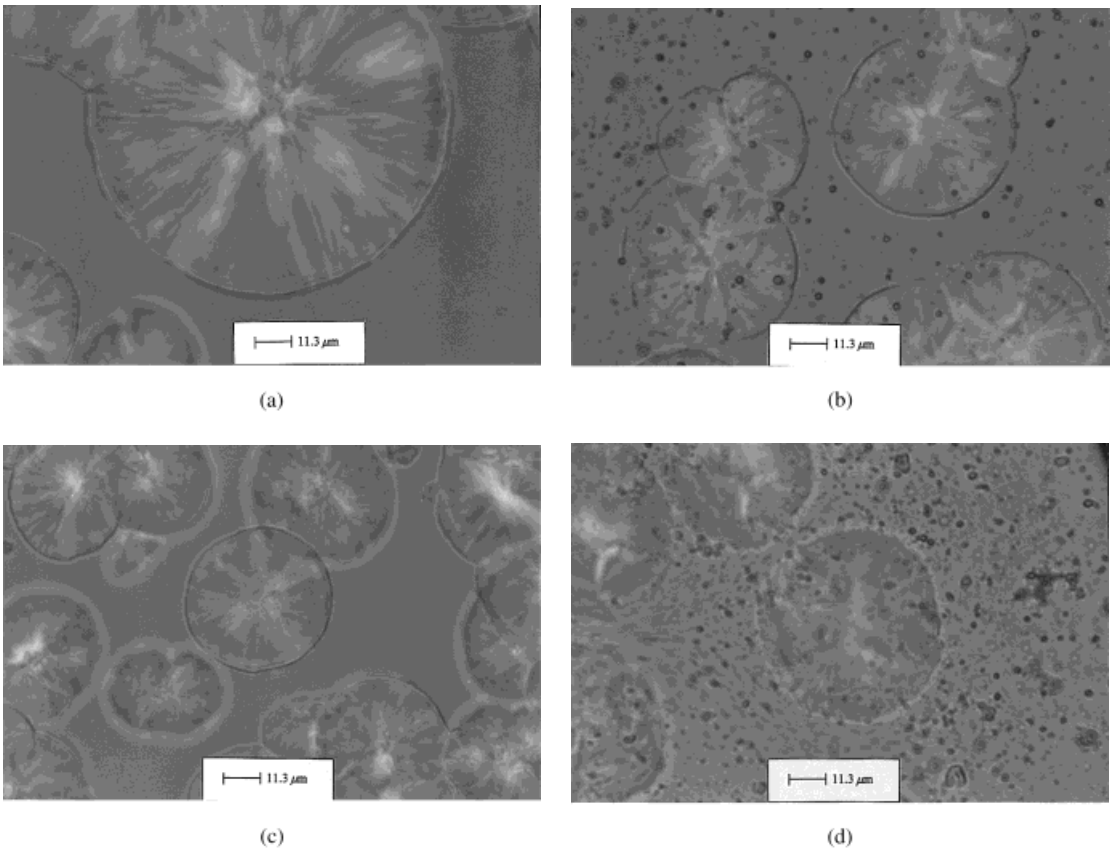

Figure 15 PLOM of some of the grafted polymers, after isothermal crystallization, at different T_cs: (a) sample PPgAM1, T_c = 133°C, ×400; (b) sample PPgAM2, T_c = 130°C, ×400; (c) sample PPgAM3, T_c = 130°C, ×400; (d) sample PPgAA, T_c = 130°C, ×400.

from the literature, that σ_e = 65–70 erg cm^{-2}. However, no reference was made regarding the M_w of their samples. It seems, therefore, that there is a tendency of σ_e to increase with the increase in M_w. The required q to bend the polymer chain back upon itself so that it can reenter the crystal also increased. This increase can be due to constraints on the chain arising when one polymer molecule simultaneously crystallizes in more than one crystallite, as Magill[17] already pointed out. If the M_w increases, the probability that the macromolecule crystallizes simultaneously in various crystallites also increases.

Regarding the heterophasic polymers, it can be observed that samples C1, C2, and C4 have similar σ_e and q values; however, sample C3 (highest percent ethene) has the highest σ_e and q. Therefore, σ_e and consequently q seem to increase with the increase in the amount of ethene (or increase in the amount of EPR). Martuscelli[20] observed this same effect: there was an increase in σ_e with the increase of the amount of rubber added to the iPP.

The σ_e and q were also found to be high for the PPgAM2.

In all of the samples, the increase of σ_e was expected because it is known that if the regularity of the polymer chain conformation on the crystalline surface decreases (by copolymerization or grafting) or if there exist constraints in the interspherulite region (promoted by the EPR particles or the MA and AA residual monomers), σ_e will increase. It is also important to point out that, for all of these calculations, a constant value of σ = 11.49 erg cm^{-2} was assumed. This is an accurate value when dealing with homopolymers; however, as we have already observed in another study on blends,[21] this value cannot be considered always constant if another polymer of similar chemical structure is present during crystallization. This value can also change if grafting occurs, for example.

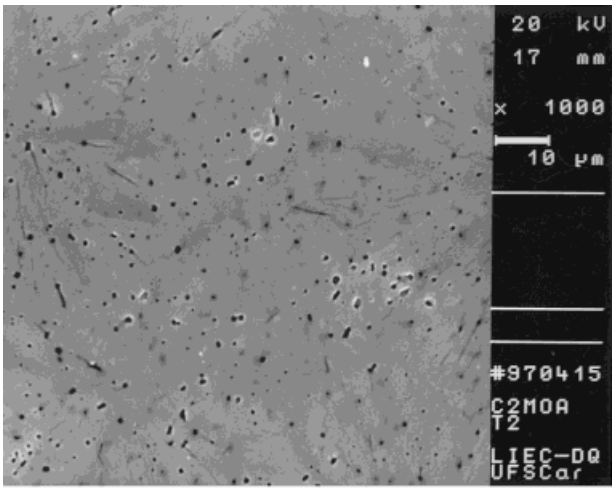

(a)

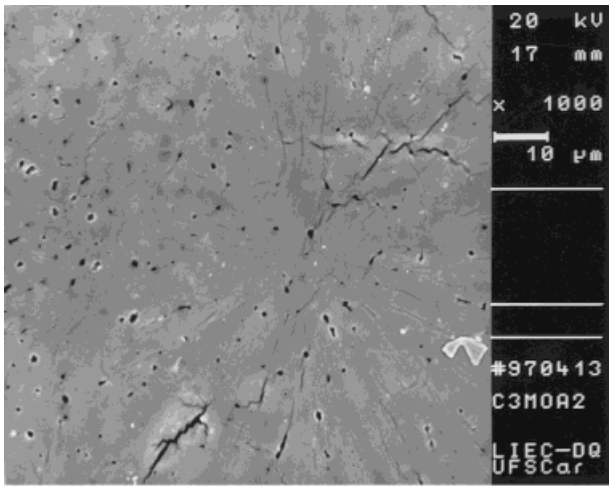

(b)

Figure 16 SEM micrographs of samples C2 and C3, after isothermal crystallization: (a) sample C2, T_c = 125°C, ×1000; (b) sample C3, T_c = 130°C, ×1000.

We can also relate G to the Avrami parameters, n and k. For homopolymers, these parameters can be calculated from the equation[11]

$$\ln[1 - X_c(t)/X_\infty] = -kt^n \qquad (8)$$

where $X_c(t)$ is the degree of crystallinity as a function of time, and X_∞ is the ultimate crystallinity at very long times.

n is related to the nucleation type and morphology developed during the crystallization, and k is related to the nucleation and growth rates (overall crystallization rate) of the crystallization.

From each isothermal crystallization run made in the DSC, $X_c(t)$ and X_∞ were calculated, and plots of $\{-\ln[1 - X_c(t)/X_\infty]\}$ as a function of crystallization time were drawn, from where n and k were computed.

Figure 9 shows the Avrami parameter k as a function of crystallization temperature for samples H1, H2, and H5. It can be observed that k increases with the decrease in crystallization temperature; at these high temperatures, the crystallization is controlled by the nucleation rate. However, sample H5 did not present the lowest k value, as it should be expected; instead, its k was the highest. We can explain this behavior by calculating the time at which 50% of the total crystallization occurred, also called half-time or $t_{1/2}$. This time was computed from the time where crystallization begun, or the induction time, t_i. The time when the temperature of the DSC reached the desired isothermal crystallization temperature was considered to be $t = 0$. Therefore, 50% of the crystallization occurred at $(t_{1/2} - t_i)$. The faster the crystallization, the lower $(t_{1/2} - t_i)$ or the higher $1/(t_{1/2} - t_i)$. Figure 10 shows these data for the same homopolymers of Figure 9.

If we compare the G data of Figure 3 with the k and $1/(t_{1/2} - t_i)$ data of Figures 9 and 10, we can observe that these values, for samples H1 and H2, behave similarly [i.e., the G, k, and $1/(t_{1/2} - t_i)$ values of sample H1 are all slightly superior to the values of samples H2], as was expected. This result indicates that the linear growth rate and the overall crystallization rate of H1 are slightly superior to the H2 rates, because this last one has a higher M_w. However, sample H5 does not follow the same trend. From Figure 3, it can be observed that its G (or linear growth rate) values are the lowest of all the samples, but its k (or its overall crystallization rate) and $1/(t_{1/2} - t_i)$ are the highest. Therefore, we can conclude that sample H5, due to its high molecular weight, also has a high nucleation rate or high nucleation density. The high molecular weight chain is capable of developing a high number of nuclei along its length. This same behavior was reported by López and Wilkes[13] on their study of the influence of M_w on the crystallization kinetics of poly(p-phenylene sulfide).

Figures 11 and 12 show k and $1/(t_{1/2} - t_i)$ for the heterophasic PP. The increase in the amount of ethene does not affect these values; however, the increase in M_w diminished these parameters, as already observed in Figure 6.

Table IV shows the Avrami parameter n for the samples. In all of the homopolymers, n was observed to increase slightly with T_c; in samples

Table V Average Size and Superficial Area of the Rubber Particles of Samples C2 and C3 as Calculated by MOCHA

Sample	C2, T_c = 125°C	C3, T_c = 130°C
Average diameter (μm)	0.6 (0.26)	0.55 (0.27)
Minimum diameter (μm)	0.01	0.19
Maximum diameter (μm)	1.06	1.27
Average area (μm^2)	0.33 (0.25)	0.3 (0.29)
Minimum area (μm^2)	0.0073	0.03
Maximum area (μm^2)	0.88	1.27
No. of particles	28	41

Numbers in parenthesis represent standard deviations.

H1 and H2, $1.5 < n < 2.0$. In sample H5, $2.1 < n < 2.7$. The higher the molecular weight, the greater the value of n. The heterophasic polymers have similar n values (average $n = 2.3$) between themselves, independent of T_c. The maleic anhydride-grafted polymer also has a value of n independent of T_c. The acrylic acid (AA)-grafted polymer showed n values higher than the PPgAM.

All of the polymers used in this study, except the PPgAA, presented a spherulitic morphology. As described previously, n can be related to the nucleation type and morphology developed during crystallization. Therefore, we would expect that samples H1 and H2 would have a diffusion-controlled crystallization with athermal or heterogeneous nucleation.[11] Sample H5 would also have a diffusion-controlled crystallization, with thermal or homogeneous nucleation.[11] However, a diffusion-controlled crystallization was not observed in these polymers.

Also, we would expect that the heterophasic polymers would have a diffusion-controlled crystallization, with homogeneous nucleation.[11] Again, this type of crystallization was not observed in these polymers.

For the grafted polymers, again a very varied morphology[11] would be expected[11]: fibrillar, circular lamellae, or truncated spheres. However, only the PPgAA sample showed a needlelike morphology.

Therefore, in general, the calculated n values did not agree with the observed experimental crystallization types.

As Jonas and Legras[22] pointed out, the Avrami parameters n and k are imprecise because of the experimental difficulties on determining t_i. In many cases, for example, these parameters are not compatible with the observed morphology obtained by PLOM. For example, in the case of the heterophasic polymers, due to the presence of the EPR particles, a heterogeneous nucleation would be expected, instead of a homogeneous[23] nucleation, as the n parameter seems to indicate.

Morphology

Figure 13 shows polarized light optical micrographs of the spherulitic morphology of some of the homopolymers after isothermal crystallization at different T_cs; the texture of the spherulites, independent of the molecular weight, is fine and the growth is radial.

Figure 14 shows micrographs of the morphology of some of the heterophasic polymers, after isothermal crystallization, also at different T_cs. The spherulite texture is gross, independent of the amount of ethene; EPR particles can be seen trapped intraspherulitically.

Figure 15 shows the morphology of some of the grafted polymers. The texture is fine and the growth is again radial; however, the PPgAA has a gross texture with needlelike structures. It can also be observed that, besides the PP crystalline structures, there exists the formation of another oilylike phase, possibly residual maleic anhydride or AA.

To calculate the average size and average area of the EPR particles in the heterophasic polymers, PLOM films were etched and observed by scanning electron microscopy as described in the Experimental section. Figure 16 presents the observed morphology of samples C2 and C3, and Table V presents the average values as calculated by MOCHA.

Figure 17 presents the particle size distribution also calculated by MOCHA. It can be observed that sample C2 had a narrow distribution curve (Poisson type), with a high percentage of particles having diameters between a narrow

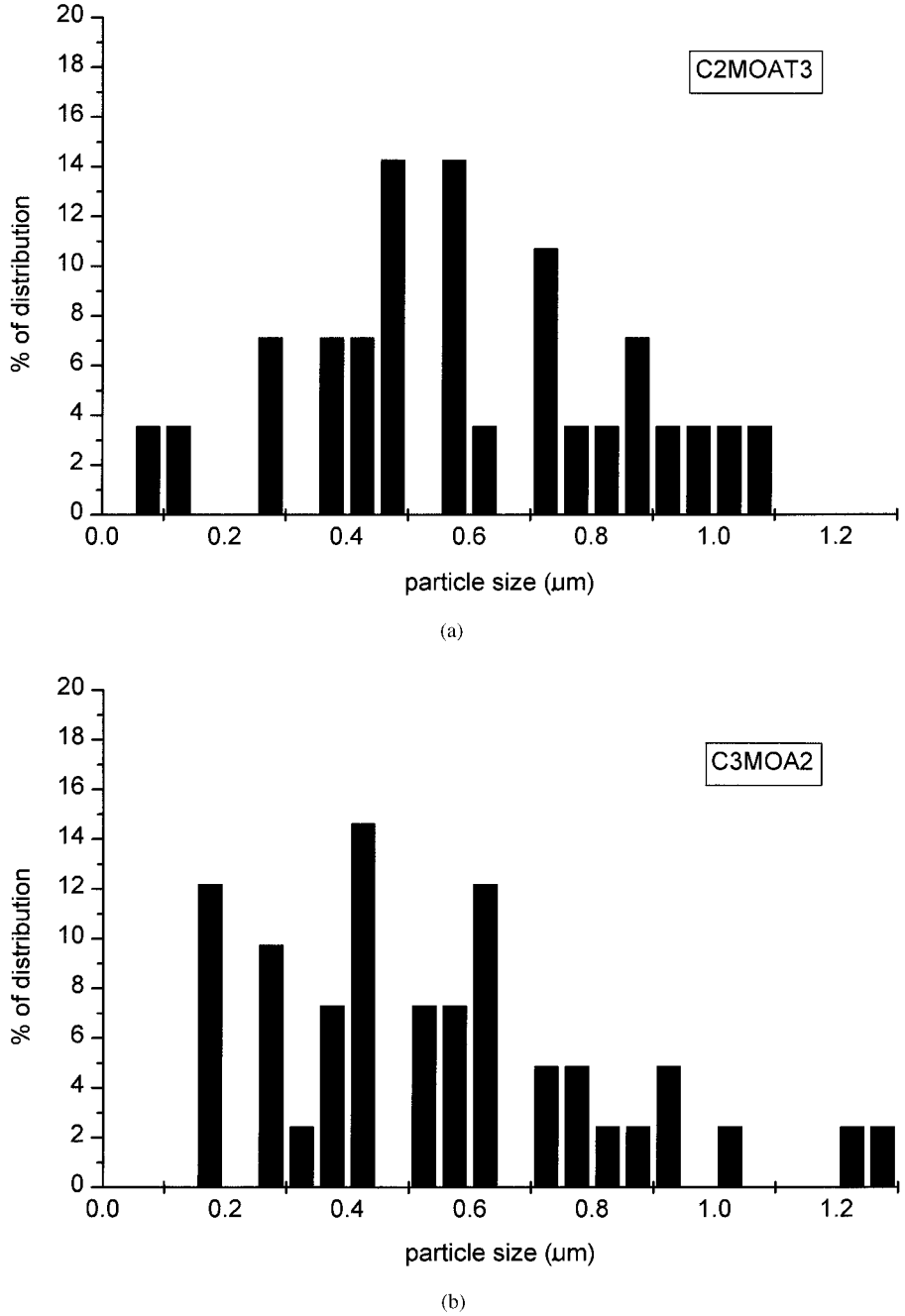

Figure 17 Particle size distribution of some of the heterophasic samples: (a) sample C2, T_c = 125°C (b) sample C3, T_c = 130°C.

range of 0.475 and 0.575 μm. This small particle size can act as a nucleating agent for crystallization, as already described. On the other side, sample C3 presented a broader distribution curve, with 73.16% of the particles having diameters between 0.175 and 0.625 μm. Because these two heterophasic polymers have different M_w and were crystallized at different T_cs, no comparison between both distributions can be made.

Finally, Figure 18 shows PLOM films of sample PPgAA as observed by scanning electron microscopy. The needlelike structures are axialites; in the interaxialite region, agglomerates, that can be attributed to residual AA, can also be observed.

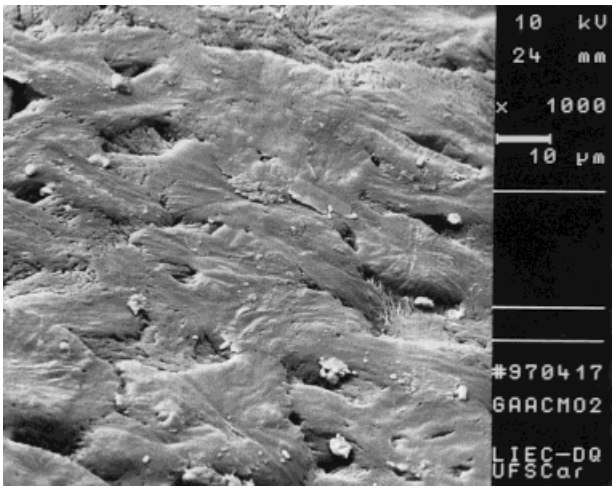

Figure 18 Scanning electron microscopic micrographs of sample PPgAA after isothermal crystallization at 130°C.

It is worthwhile to point out that axialites are predecessor structures to the spherulites; therefore, probably the complete formation of spherulites was avoided by the presence of residual AA.

CONCLUSIONS

The following conclusions can be inferred from this work.

For all of the samples, the spherulite growth rate was not controlled by diffusion. The linear growth rate G decreased with the increase of the molecular weight of the homopolymers. For the heterophasic polymers, the ones with similar M_w had their G increased as the amount of ethene increased. However, when the M_w increased, its effect on G outstripped the effect promoted by the amount of ethene. In the grafted polymers, as the amount of grafting increased, G decreased.

Data of G as a function of temperature were fitted by using the Lauritzen and Hoffman equation for all of the samples. The σ_e values of the lower molecular weight homopolymers were similar to the ones found in the literature. However, these values increased with the increase in M_w. Also, the heterophasic and grafted polymers had values of σ_e higher than homopolymers.

The homopolymer H5 had an overall rate of crystallization higher than of the lower molecular weight homopolymer; however, its G was the lowest. This can be a consequence of a higher nucleation density, due, for example, to the increase in the amount of intramolecular folded chain nuclei.[11] The amount of ethene and grafting did not influence the overall rate of crystallization of the heterophasic and grafted polymers.

The calculated Avrami parameter n for all of the samples was between $1.5 < n < 2.7$, suggesting a diffusion-controlled crystallization with spherulitic morphology. By PLOM, the observed morphology was spherulitic in all cases, except for the PPgAA polymer, which presented a needle-like structure. However, as described previously, no diffusion-controlled crystallization was observed.

The heterophasic polymers had an average particle size of 0.55–0.6 μm; sample C2 after crystallizing at 125°C, had a narrow distribution of particle sizes, whereas sample C3, after crystallizing at 130°C, had a broad distribution of particle sizes.

The PPgAA sample presented an axialite morphology, with residual AA agglomerates in the interaxialites region.

The authors wish to express their gratitude to OPP Petroquímica do Brasil, FAPESP 94/2317-9, CNPq, and Volkswagen Fundation of Germany (I-69693) for financial support and to Humberto Bezerra for help with the experimental work.

REFERENCES

1. J. M. Charrier, *Polymeric Materials and Processing,* Hanser Publishers, New York, 1990.
2. A. I. Isayev, T. W. Chan, M. Gmerek, and K. Shimojo, *J. Appl. Polym. Sci.,* **55,** 821 (1995).
3. A. I. Isayev, T. W. Chan, K. Shimojo, and M. Gmerek, *J. Appl. Polym. Sci.,* **55,** 807 (1995).
4. G. Eder, H. Janeschitz-Kriegl, and S. Liedauer, *Progr. Polym. Sci.,* **15,** 629 (1990).
5. E. J. Clark and J. D. Hoffman, *Macromolecules,* **17,** 87 (1984).
6. J. D. Hoffman, G. T. Davis, and J. I. Lauritzen, Jr., in *Treatise on Solid State Chemistry,* Vol. 3, N. B. Hannay, Ed., Plenum Press, New York, 1976, Chap. 7.
7. J. Varga, *J. Mat. Sci.,* **27,** 2557 (1992).
8. M. Yamaguchi, H. Miyata, and K. Nitta, *J. Polym. Sci. Part B: Polym. Phys.,* **35,** 953 (1997).
9. G. B. A. Lim, K. S. McGuire, and D. R. Lloyd, *Polym. Eng. Sci.,* **33,** 9 (1993).
10. C. A. Hieber, *Polymer,* **36,** 1455 (1995).
11. B. Wunderlich, *Macromolecular Physics,* Vol. 2, Academic Press, New York, 1976, p. 147.

12. T. S. Dziemianowicz and W. W. Cox, *Proceedings, ANTEC '85,* 540, 1985.
13. L. C. López and G. L. Wilkes, *Polymer,* **29,** 106 (1988).
14. S. Misra, F. M. Lu, J. E. Spruiell, and G. C. Richeson, *J. Appl. Polym. Sci.,* **56,** 1761 (1995).
15. J. D. Hoffman and R. L. Miller, *Macromolecules,* **21,** 3038 (1988).
16. L. Pospisil and F. Rynikar, *Polymer,* **31,** 476 (1990).
17. J. H. Magill, *J. Polym. Sci., Part A-2,* **5,** 9 (1967).
18. J. P. Runt and L. M. Martynovicz in *Multicomponent Polymer Materials, Adv. Chem. Ser.,* D. R. Paul and L. H. Sperling, Eds., American Chemical Society, Washington, DC, 1986.
19. L. H. Sperling, *Introduction to Physical Polymer Science,* 2nd ed., Wiley-Interscience Publishers, New York, 1992.
20. E. Martuscelli, *Polym. Eng. Sci.,* **24,** 563 (1984).
21. B. Carvalho and R. E. S. Bretas, *J. Appl. Polym. Sci.,* **55,** 233 (1995).
22. A. Jonas and R. Legras, *Polymer,* **32,** 2691 (1991).
23. W. Weng and M. Asresahegn, *Polym. Eng. Sci.,* **33,** 877 (1993).